NASA/TM—2003-212379

Numerical and Experimental Determination of the Geometric Far Field for Round Jets

L. Danielle Koch, James Bridges, and Cliff Brown
Glenn Research Center, Cleveland, Ohio

Abbas Khavaran
QSS Group, Inc., Cleveland, Ohio

May 2003

The NASA STI Program Office . . . in Profile

Since its founding, NASA has been dedicated to the advancement of aeronautics and space science. The NASA Scientific and Technical Information (STI) Program Office plays a key part in helping NASA maintain this important role.

The NASA STI Program Office is operated by Langley Research Center, the Lead Center for NASA's scientific and technical information. The NASA STI Program Office provides access to the NASA STI Database, the largest collection of aeronautical and space science STI in the world. The Program Office is also NASA's institutional mechanism for disseminating the results of its research and development activities. These results are published by NASA in the NASA STI Report Series, which includes the following report types:

- TECHNICAL PUBLICATION. Reports of completed research or a major significant phase of research that present the results of NASA programs and include extensive data or theoretical analysis. Includes compilations of significant scientific and technical data and information deemed to be of continuing reference value. NASA's counterpart of peer-reviewed formal professional papers but has less stringent limitations on manuscript length and extent of graphic presentations.

- TECHNICAL MEMORANDUM. Scientific and technical findings that are preliminary or of specialized interest, e.g., quick release reports, working papers, and bibliographies that contain minimal annotation. Does not contain extensive analysis.

- CONTRACTOR REPORT. Scientific and technical findings by NASA-sponsored contractors and grantees.

- CONFERENCE PUBLICATION. Collected papers from scientific and technical conferences, symposia, seminars, or other meetings sponsored or cosponsored by NASA.

- SPECIAL PUBLICATION. Scientific, technical, or historical information from NASA programs, projects, and missions, often concerned with subjects having substantial public interest.

- TECHNICAL TRANSLATION. English-language translations of foreign scientific and technical material pertinent to NASA's mission.

Specialized services that complement the STI Program Office's diverse offerings include creating custom thesauri, building customized databases, organizing and publishing research results . . . even providing videos.

For more information about the NASA STI Program Office, see the following:

- Access the NASA STI Program Home Page at ***http://www.sti.nasa.gov***

- E-mail your question via the Internet to help@sti.nasa.gov

- Fax your question to the NASA Access Help Desk at 301–621–0134

- Telephone the NASA Access Help Desk at 301–621–0390

- Write to:
  NASA Access Help Desk
  NASA Center for AeroSpace Information
  7121 Standard Drive
  Hanover, MD 21076

NASA/TM—2003-212379

Numerical and Experimental Determination of the Geometric Far Field for Round Jets

L. Danielle Koch, James Bridges, and Cliff Brown
Glenn Research Center, Cleveland, Ohio

Abbas Khavaran
QSS Group, Inc., Cleveland, Ohio

Prepared for
Noise-Con 2003
sponsored by the Institute of Noise Control Engineering of the USA (INCE-USA)
Cleveland, Ohio, June 23–25, 2003

National Aeronautics and
Space Administration

Glenn Research Center

May 2003

Available from

NASA Center for Aerospace Information
7121 Standard Drive
Hanover, MD 21076

National Technical Information Service
5285 Port Royal Road
Springfield, VA 22100

Available electronically at http://gltrs.grc.nasa.gov

NUMERICAL AND EXPERIMENTAL DETERMINATION OF THE GEOMETRIC FAR FIELD FOR ROUND JETS

L. Danielle Koch, James Bridges, and Cliff Brown
National Aeronautics and Space Administration
Glenn Research Center
Cleveland, Ohio

Abbas Khavaran
QSS Group, Inc
Cleveland, Ohio

Abstract

To reduce ambiguity in the reporting of far field jet noise, three round jets operating at subsonic conditions have recently been studied at the NASA Glenn Research Center. The goal of the investigation was to determine the location of the geometric far field both numerically and experimentally. The combination of the WIND Reynolds-Averaged Navier-Stokes solver and the MGBK jet noise prediction code was used for the computations, and the experimental data was collected in the Aeroacoustic Propulsion Laboratory.

While noise sources are distributed throughout the jet plume, at great distances from the nozzle the noise will appear to be emanating from a point source and the assumption of linear propagation is valid. Closer to the jet, nonlinear propagation may be a problem, along with the known geometric issues. By comparing sound spectra at different distances from the jet, both from computational methods that assume linear propagation, and from experiments, the contributions of geometry and nonlinearity can be separately ascertained and the required measurement distance for valid experiments can be established.

It is found that while the shortest arc considered here (~8D) was already in the geometric far field for the high frequency sound (St >2.0), the low frequency noise due to its extended source distribution reached the geometric far field at or about 50D. It is also found that sound spectra at far downstream angles does not strictly scale on Strouhal number, an observation that current modeling does not capture.

Introduction

Jet noise remains a difficult engineering challenge today partly because, unlike many other fields of engineering, jet noise does not have the fundamental formulas and predictive equations that can be solved numerically on a computer. Once the relationships between flow and sound have been established we will be able to take advantage of the rapidly increasing power of computers to design quiet propulsion systems for aircraft. Until we can solve for jet noise directly, we use approximate methods to guide our designs and gain insight into the features of the flow that affect noise generation and propagation. Through studies like the one in the present paper, NASA Glenn is currently assessing the suitability of the WIND code for producing calculated mean flows from single and separate flow jets and using these computational fluid dynamics (CFD) solutions as the input for physics-based aeroacoustic prediction methods such as MGBK.

In working to achieve this noise prediction system it is critical to validate the CFD and jet noise models separately against good experimental data. Measuring turbulence from jets is extremely challenging. Recently, Particle Image Velocimetry (PIV) has come to be a valuable tool for collecting turbulence data which is being used for validation of the mean flow predictions. Acquiring high quality acoustic data to use for validation of the acoustic predictions would seem to be easier, but in fact there are several ways in which experimental jet noise can be deficient.

One of the ways jet noise can be misleading is by being acquired in the geometric near field of the jet. (Ref. 1) Since it is expensive to have a large enough anechoic chamber for jet work, often the measurements are made relatively close to the jet and extrapolated to far field assuming a point source and projecting out using spherical spreading. The main problem here is that the source region is large in a jet and until the observer is very far away this source cannot be treated as a point. A second potential problem is that near-field sound levels in larger jets are above that commonly thought to have purely linear propagation. Determining how much of an effect this has on the scalability of jet noise data is not easy.

A special test was done at NASA Glenn to address the question, “How close is too close?” The noise prediction tools developed to date were exercised on the same conditions to differentiate linear and nonlinear propagation issues, since the prediction tools strictly use linear propagation methods. This also allowed comparison of how well accepted jet noise scaling laws were obeyed in both experimental data and

computational predictions. By looking at jet noise data at 90° and 150° we are evaluating the predictive method where it is thought to work the best and the worst, respectively.

Description of Aerodynamic and Acoustic Measurements

Measurements were made using the Small Hot Jet Acoustic Rig (SHJAR) (Fig. 1) at the NASA Glenn Research Center's Aero Acoustic Propulsion Laboratory (AAPL). The AAPL is a geodesic dome 65 feet in radius with acoustic treatment producing an anechoic environment down to 200Hz. SHJAR is a single flow jet facility capable of operating a nozzle, nominally 51mm in diameter over a flow range up to Mach 2 and temperatures up to 1000 K. The jet centerline is 10 feet above the concrete floor, over 7 feet above the anechoic wedges. By rigorous checkout using multiple size nozzles, the rig has been determined to be free from internal rig noise for a 51mm nozzle down to roughly M=0.3 cold flow condition. The nozzles used for this test had three different exit diameters: 1 in (25.4mm), 2 in (51mm), and 3 in (76.2mm). They were designed to have similar characteristics: inlet diameter (152mm), lip thickness (1.3mm), outside face angle (30° to jet axis), and parallel flow section at the exit (6.4mm).

Far-field acoustic measurements were made using three B&K 3934 microphones on poles at the jet centerline height. One microphone was placed at a reference position well away from the jet while the other two were manually moved along radial lines 90° and 150° from the jet upstream axis. Thus, acoustic data was acquired for 12 different distances from 8 to 100 jet diameters. All acoustic data was processed as narrowband spectra before being integrated to third octave bands for plotting.

In this paper we will be presenting two cold jet conditions tested for the 2 in and 3 in nozzles: $M_j = U_j/a_\infty = 0.5, 0.9$. This data will be used to validate the aerodynamic predictions from the WIND code and the acoustic predictions from MGBK as part of the ongoing determination of the suitability of the WIND/MGBK suite for jet noise prediction.

Description of Aerodynamic Predictions

The aerodynamic predictions of the mean flow from these nozzles were generated using the WIND code (version 4.136). WIND is a general purpose Reynolds-Averaged Navier-Stokes solver. Development of the WIND code continues through efforts of the NPARC Alliance, a partnership between the NASA Glenn Research Center and the Arnold Engineering Development Center [Ref. 2]. The NPARC Alliance strives to make WIND a flexible, applications-oriented solver. WIND gains its flexibility by being able to obtain steady-state or time-accurate simulations for a variety of realistic applications modeled with axisymmetric, 2- or 3-dimensional multiblock structured grids. Convergence acceleration can be achieved through parallel processing and grid sequencing

For the present simulations, multiblock axisymmetric structured grids were created for the 1, 2, and 3 inch nozzles tested in the Aeroacoustic Propulsion Laboratory. Each grid extended 75 jet diameters downstream of the nozzle exit plane and 25 jet diameters radially outward from the jet centerline. The total number of gridpoints varied between the grids for the 1, 2 and 3 inch nozzles in an effort to reduce stretching. The total number of gridpoints for the 1 in nozzle was 12,543. The total number of gridpoints for the 2 in nozzle was 32,895, and the total number of gridpoints for the 3 in nozzle was 66,615. The detail of the grid for the 2 inch nozzle is shown in Figure 2 accompanied by the variation of $y^+ \left(y^+ = \frac{y}{\nu_w}\sqrt{\frac{\tau_w}{\rho_w}} \right)$ for the first gridline off the inner jet wall for all simulations. The maximum value for y^+ of the first gridline off the wall did not exceed 9 for any of the cases. Viscous wall boundary conditions were applied to the inner nozzle wall, while inviscid surface boundary conditions were applied to the outer wall, nozzle blunt edge, and jet centerline boundary. Freestream conditions were applied at the far radial boundary, while total temperatures and total pressures were held constant at the inlet planes and a static pressure constraint was applied at the outflow boundary. The value for the turbulent Prandtl number was set equal to a constant of 0.72. The freestream Mach number for all cases was 0.05.

Using the Menter SST turbulence model to initialize the flow on the coarse grid for the first 5000 cycles, the Chien κ-ϵ turbulence model was used to obtain the converged solution on the fine grid. No compressibility corrections were used. Both centerline axial velocity and lipline turbulence kinetic energy distributions were monitored to determine convergence, in addition to the L2 residuals.

Description of Acoustic Predictions

With advances in computer power, direct numerical simulation (DNS) is making headway in simulation of aerodynamic noise for very simple geometries. But, as long as these simulations continue to be prohibitively expensive and time consuming semi-empirical methods combined with experimental

observations remain the tool of choice in propulsion noise studies.

The current version of the MGBK jet noise prediction methodology has its origins in a unified aeroacoustics model (MGB) developed by the General Electric company [Ref. 3]. In general, linearized inhomogeneous equations of motion for an inviscid flow (viscous effects are usually neglected) describe generation as well as propagation of sound through a steady mean flow. These equations may be combined to form a single third-order wave equation also known as Lilley's equation [Ref. 4]. Once the operator part of this equation is linearized the sound field may be estimated using the superposition principle. It is convenient to linearize the equation about a locally parallel base flow as is done in the MGBK methodology. The non-linear terms are now moved to the right hand side of the equation and are identified as the source. With x_1 pointed in the direction of the mean axial velocity U it is shown that

$$L\Pi \cong \frac{D}{Dt}\frac{\partial f_i}{\partial x_i} - 2\frac{\partial U}{\partial x_i}\frac{\partial f_i}{\partial x_1}$$

where L is Lilley operator, $\Pi \equiv p'/(\gamma p_o)$ is identified with acoustic pressure fluctuations p', $D/Dt \equiv \partial/\partial t + U\partial/\partial x_1$, t is time, and p_o denotes a constant static pressure. Here u_i denotes turbulent velocity component and $f_i \equiv \partial(u_i u_j)/\partial x_j$. Source terms appearing in the right hand side of the above equation are both second order in velocity fluctuations and are designated as self- and shear-noise source terms respectively. Additional sources due to density fluctuations are neglected hereon. Sound spectral density in the far field may be written as integration with respect to the jet volume of source density multiplied by an appropriate Green's function. In describing the source, fourth-order velocity correlations are usually expressed in terms of second order ones using quasi-normal approximation. The second-order correlations are modeled using appropriate spatial and temporal functions. These models should be consistent with requirements of a locally homogeneous, quasi-incompressible isotropic (or axisymmetric) turbulence [Ref. 5].

The mean flow used by MGBK as input can be obtained from a Reynolds-Averaged Navier-Stokes (RANS) or an Algebraic Stress Model (ASM). The latter has the advantage of providing component stresses that could be used in an axisymmetric turbulence model. When using RANS type calculations, factors ($\overline{u_2^2}/\overline{u_1^2}$) relating the turbulence components, and (ℓ_2/ℓ_1) associated with length-scales may be introduced universally for the entire jet. Here subscripts 1 and 2 refer to stream- and span-wise directions respectively. Length- and time-scales of turbulence (i.e. ℓ_1 and τ_o) are calculated from $\ell_1 \sim \kappa^{3/2}/\varepsilon$ and $\tau_o \sim \kappa/\varepsilon$ where κ and ε denote the turbulence kinetic energy and its dissipation rate, respectively.

The Green's function governing the above equation describes the effect of the surrounding mean flow on radiated sound. Mean velocity gradients and temperature gradients are known to refract the acoustic energy within the shear layer.

Once beyond the jet boundary, sound propagates according to a free-space Green's function $\exp(ikR)/(4\pi R)$ where R is the distance from the source, $k \equiv \omega/c$ is the wave number and ω is frequency. The familiar inverse-square law is thus used for distance scaling of sound intensity. It should be noted that this law applies only when the source region is limited in extent. For a typical jet, the more active source region usually extends a number of jet diameters, say 10 to 15, from the jet exit. However, if the observer is located far enough away relative to exit diameter (i.e., $R/D >> 1$), the inverse-square law may be applied to scale the sound for additional distance. The minimum distance required to treat the source as a point source is usually referred to as the geometric far field (GFF).

In addition to distance scaling, the atmospheric absorption coefficient [Ref. 6] should be applied in the usual way to attenuate the high frequency sound with distance. Noise measurements usually reflect atmospheric attenuation and a lossless spectrum is calculated using the attenuation law.

When a jet is axisymmetric, the Green's function may be calculated using the properties of the cylindrical functions. In the current MGBK predictions the Green's function is calculated using a high frequency solution known as a quasi-symmetric approximation. This solution usually deteriorates close to the boundary of zone of silence that forms near the downstream jet axis. A more rigorous high frequency solution, referred to as an asymmetric approximation [Ref. 7] produces better agreement with the exact solution and is under consideration for future improvement of the MGBK code.

The analysis of [Ref. 5] indicates that sound spectral intensity scales with turbulence kinetic energy as ($\sim \kappa^{7/2}$). Furthermore, in the acoustically active regions of the jet, turbulence kinetic energy scales with exit jet velocity as $\kappa \sim U_j^2$. Lighthill's theory [Ref.8] states that at low Mach numbers, the total acoustic power radiated from a jet scales with exit velocity as U_j^8. We will investigate the location of the geometric far field as well as Lighthill's power law for the jets

considered in this exercise when discussing the MGBK results.

Examination of Aerodynamic Results

Since we have used WIND and MGBK together, accurate noise predictions hinge on accurate mean flow predictions. PIV data from the 1 and 2 inch nozzles are used to validate the mean flow predictions (Ref. 9). Figure 3 is a comparison of the measured and predicted axial velocity distributions for all three jets (1, 2, and 3 in) at Mach 0.9. The axial velocity has been normalized by the centerline exit plane velocity and the distances are normalized by the respective jet diameter. There is good agreement between the measured and predicted potential core lengths.

Similarly, Figure 4 shows the measured and predicted levels of turbulence kinetic energy. Turbulence kinetic energy has been normalized by the square of the centerline exit plane velocity, and distances have once again been normalized by the respective jet diameter.

Turbulence kinetic energy is calculated from instantaneous velocity measurements obtained from the PIV system described earlier. The equation for turbulence kinetic energy, κ, is [Ref. 10]:

$$\kappa = \frac{1}{2}\left[\overline{u_1 u_1} + \overline{u_2 u_2} + \overline{u_3 u_3}\right]$$

If axisymmetric turbulence is assumed, $\overline{u_3 u_3}$ can be approximated by $\overline{u_2 u_2}$ in the equation above, where $\overline{u_1 u_1}$ and $\overline{u_2 u_2}$ are the variances of the measured velocities in the axial and radial directions, respectively. Predicted turbulence kinetic energy is found from the Chien k-ϵ equations implemented in the WIND code, as described in Reference 11. Since turbulence kinetic energy found from two-equation turbulence models is derived from Favre-averaged variables by dividing squares of momentum by the square of density, comparisons of turbulence kinetic energy from CFD and PIV are not exact. Even so, comparisons of predicted and measured turbulence kinetic energy show reasonable agreement. Unlike the comparisons of axial velocity, there does appear to be some variation of the distribution of turbulence kinetic energy between the normalized predictions and measurements, with the areas of maximum turbulence kinetic energy growing larger as jet diameter increases.

Examination of Acoustic Results

RANS solutions from the WIND solver for Mach 0.5 and 0.9 isothermal jets are used as input to MGBK noise predictions. Three jet diameters (D =1, 2 and 3 in) are considered in each case. The observer distance is varied according to Table 1 in order to demonstrate the location of the geometric far field and additionally investigate Lighthill's power law as discussed earlier. All noise plots are shown as lossless.

Figure 5 shows 90° spectral predictions, now scaled to a distance of 100D for each jet using inverse-square law. It is clear that at a Strouhal number larger than 2.0 ($St \equiv fD/U_j$) the spectra collapse quite well for each nozzle, indicating that every distance listed in Table 1 is the GFF for this range of frequency. This confirms the general belief that the high-frequency sources are primarily distributed close to the jet exit. Low frequency noise sources, on the other hand, extend farther downstream and require more distance to reach the GFF. This is indicated by slight variation in noise level at the low frequency segment of each prediction. Beyond 50D even the low frequency segment of various predictions collapse completely, thus 50D places each prediction in the GFF for the entire range of its spectrum.

Table 1.—Microphone Locations

R/D	2 in nozzle, R, in	3 in nozzle, R, in	Plotted on Fig. 5,7,9,11
7.9	15.9	23.8	No
10.0	20.0	30.0	Yes
12.6	25.2	37.8	No
15.8	31.7	47.5	No
20.0	39.9	59.9	Yes
25.1	50.2	75.4	No
31.6	63.2	94.9	No
39.8	79.6	119.4	No
50.1	100.2	150.4	Yes
63.1	126.2	189.3	No
79.4	158.9	238.3	No
100.0	200.0	300.0	Yes
500.0	1000.0	1500.0	Fig. 5 and 9 only

To investigate the power law, the GFF prediction for each nozzle (at R/D=50) was scaled according to the U^8 law. Shown in Figure 6 are results at 90°. It is seen that while the agreement with the 8th power law is relatively satisfactory, still the two Mach numbers do not collapse completely. Figure 7 is similar to Figure 5 and shows the measured spectra at 90° scaled to 100D for the 2 and 3 inch nozzles. Figure 8 is similar to Figure 6 and shows the measured noise spectra at R/D=50 from Figure 7 additionally scaled by the 8th power law. Measurements of Figure 8 show a better conformity with 8th power law. Note that the 2 in nozzle data differs from the 3 in at high frequencies at M=0.5, an artifact apparently related to the lower

Reynolds number of the nozzle and not deemed to be characteristic of high Reynolds number jets.

Figures 9 through 12 show similar results at 150° from the jet inlet. The 8th power law (Figures 10 and 12) does not completely collapse the spectra from different Mach numbers. Historically, an additional factor, a Doppler factor of $(1-M_c \cos\theta)^{-5}$ is included to bring these data together, where $M_c = 0.6*M_j$. There is also a variation in the peak frequency of spectra at the two Mach numbers as seen in the measurements of Figure 12. It appears that the location of the peak at this particular angle might better scale with the Helmholtz number ($He \equiv f D / c$). This effect is not found in the predictions although they do not obey strict Strouhal scaling, presumably because of Mach number dependent refraction effects.

Comparison between prediction and measurement for the above two Mach numbers is shown in Figures 13 and 14. At 90°, refraction effects are absent and any deficiency in prediction may directly be attributed to the source modeling. It is argued [Ref. 12] that modeling the source via an exponential spatial function (in place of the Gaussian model in the MGBK methodology) predicts a broader spectrum and a better agreement with 90° measurements. On the other hand, 150° is the vicinity of the peak directivity angle, which also coincides with the boundary of the zone of silence. A good prediction at this angle, additionally, is particularly sensitive to the accuracy of the Green's function. Reference [Ref. 7] shows that an asymmetric Green's function improves predictions at and near the zone of silence relative to the quasi-symmetric Green's function employed in the current MGBK predictions.

Conclusions

Two isothermal subsonic jets at Mach numbers of 0.5 and 0.9 were considered in this study. In the first part, measurements as well as predictions show that in order to properly measure jet noise microphones must be placed at least 50 jet diameters away from the nozzle exit plane. Additionally, it was shown that the high frequency sound, due to its limited extent, reached its geometric far field at a much shorter distance.

The combination of WIND and MGBK has so far proven to be a useful tool for predicting jet noise at 90°, though NASA's assessment of these tools continues. Results have shown that while the predicted and measured sound spectra scale with classic 8th power law and Strouhal number at a 90° radiation angle, closer to the jet axis at 150°, the Strouhal scaling is less satisfactory. For now it appears that the frequency scales better with Helmholtz number, although this may be a fortuitous result of the change in refraction with Mach number that is not currently being computed accurately in the predictions. Finally, no nonlinear propagation effect could be discerned from this data; in fact the trends appear to indicate that the effect is relatively insignificant.

REFERENCES

[1] Ahuja, K. K., "Designing Clean Jet Noise Facilities and Making Accurate Jet Noise Measurements," AIAA 2003-0706.

[2] Bush, R. H., G. D. Power, and C. E. Towne, "WIND: The Production Flow Solver of the NPARC Alliance," AIAA-98-0935.

[3] R. Mani, P. R. Gliebe, and T. F. Balsa, "High Velocity Jet Noise Source Location and Reduction," *FAA-RD-76-79-II*, 1978.

[4] G. M. Lilley, *AGARD-CP-131*, pp. 13.1-13.12, 1974.

[5] A. Khavaran, "Role of Anisotropy in Turbulence Mixing Noise," AIAA J., **37(7)**, pp. 832-841, 1999.

[6] H. E. Bass, L. C. Sutherland, A. J. Zuckerwar, D. T. Blactock and D. M. Hester, "Atmospheric Absorption of Sound: Further Development," J. Acoust. Soc. Am. **97**, pp. 680-683, 1995.

[7] D. W. Wundrow, and A. Khavaran, "On the Application of High-Frequency Approximation to Lilley's Equation," *NASA/CR-2003-212089*, 2003.

[8] M. J. Lighthill, "On Sound Generated Aerodynamically: Turbulence as a Source of Sound," Proc. Roy. Soc. Lon., A222, pp. 1-32, 1954.

[9] Bridges, J. and Wernet, M. P., "Measurements of the Aeroacoustic Sound Source in Hot Jets," AIAA-2003-3130

[10] Wilcox, D. C., Turbulence Modeling for CFD, Second Edition, DCW Industries, Inc. 2000.

[11] Yoder, D. A., N. J. Georgiadis, "Implementation and Validation of the Chien κ-ϵ Turbulence Model in the Wind Navier Stokes Code," AIAA 99-0745

[12] A. Khavaran, and J. Bridges, "A Parametric Study of Fine-Scale Turbulence Mixing Noise," AIAA-2002-2419, 2002.

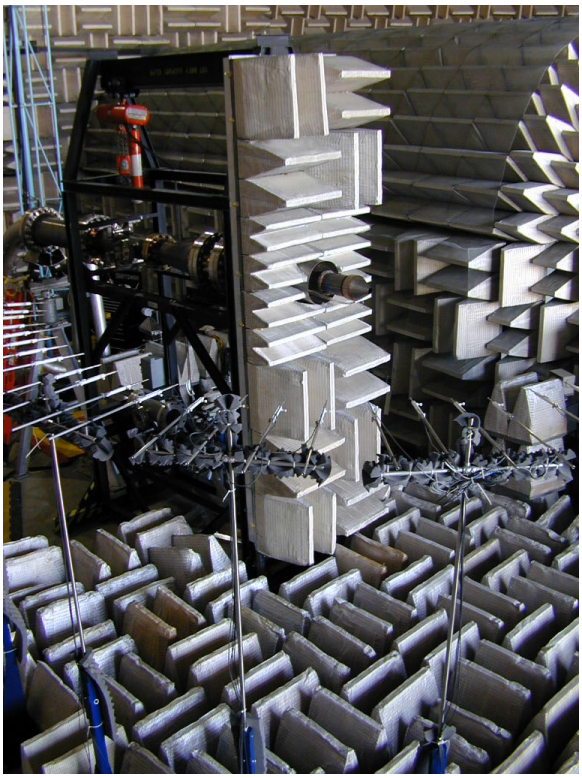

Figure 1.—Small Hot Jet Acoustic Rig (SHJAR) in the NASA Glenn Aeroacoustic Propulsion Lab

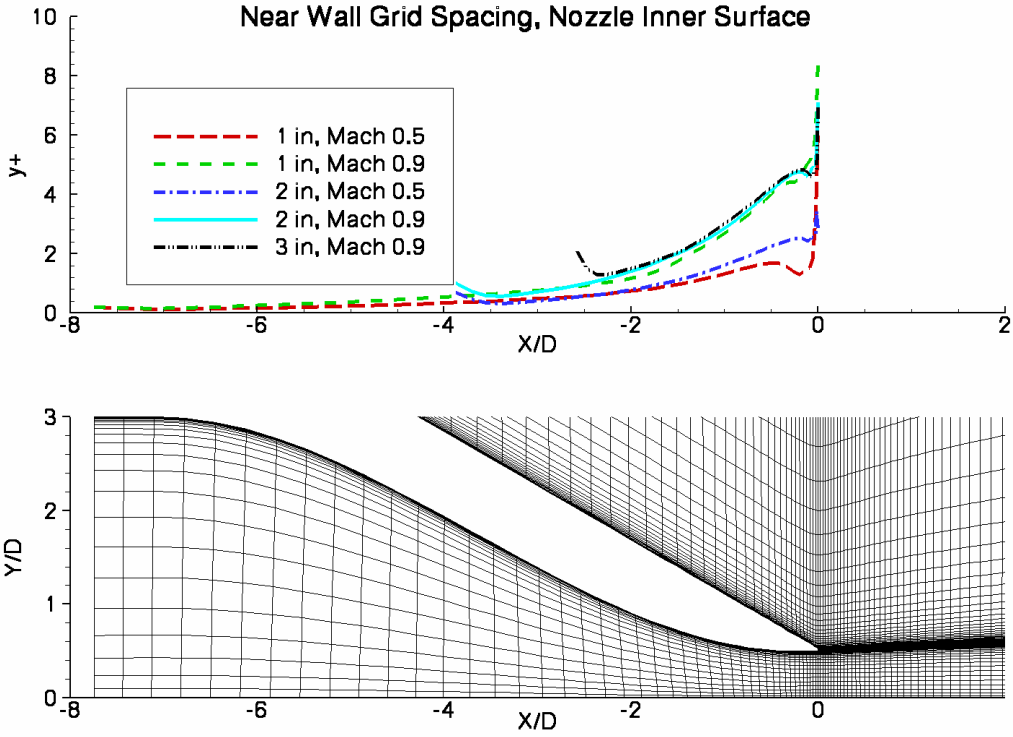

Figure 2.—Detail of computational grid for the 2 inch nozzle, and variation of y^+ as a function of axial distance for all cases.

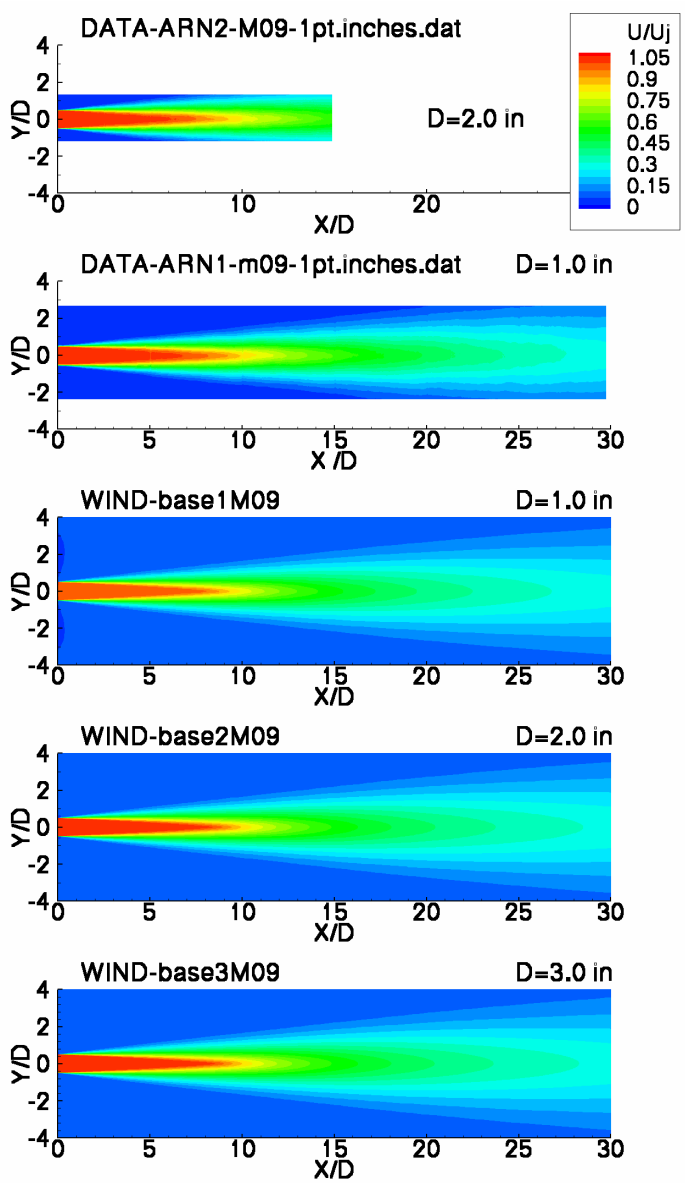

Figure 3.—Normalized Axial Velocity Distributions, Mach 0.9

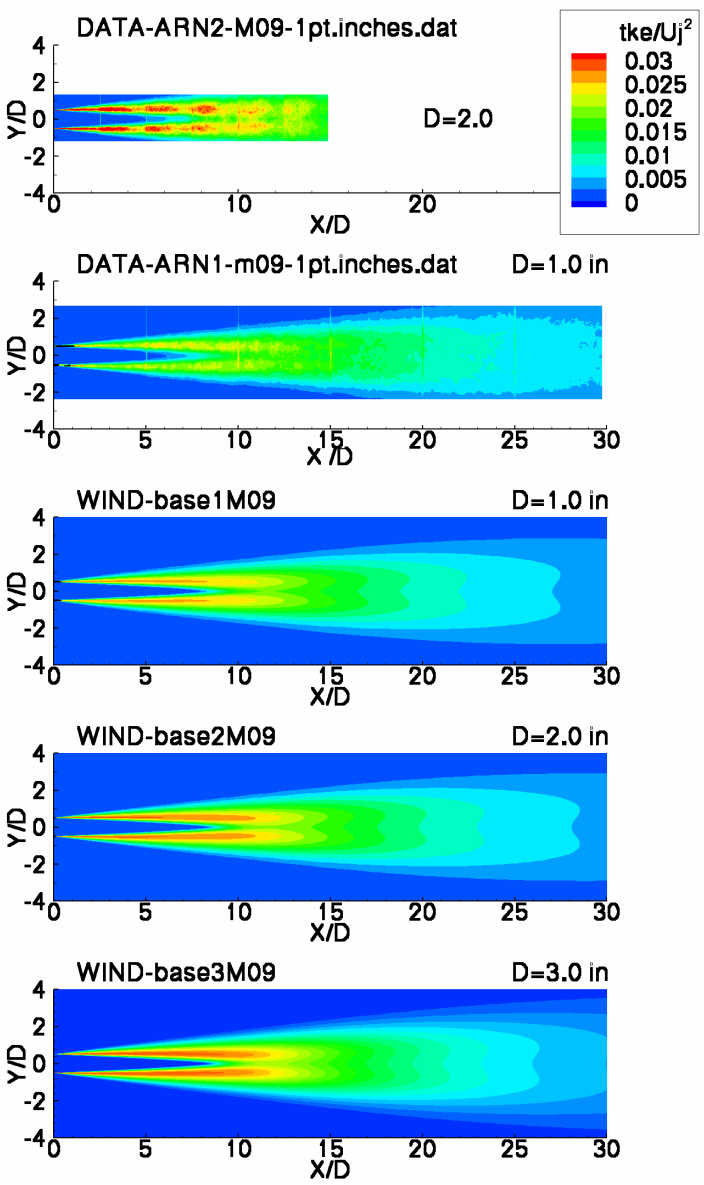

Figure 4.—Normalized Turbulence Kinetic Energy Distributions, Mach 0.9

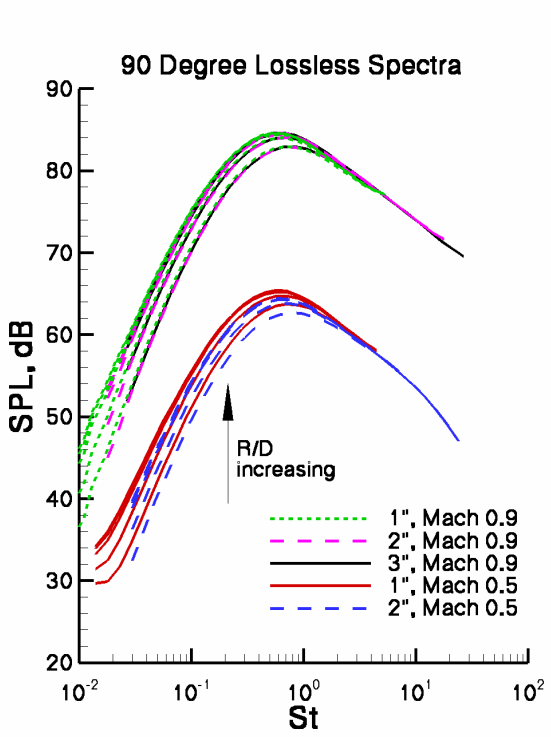

Figure 5.—Predicted spectra at 90° scaled to 100 diameters using inverse square law

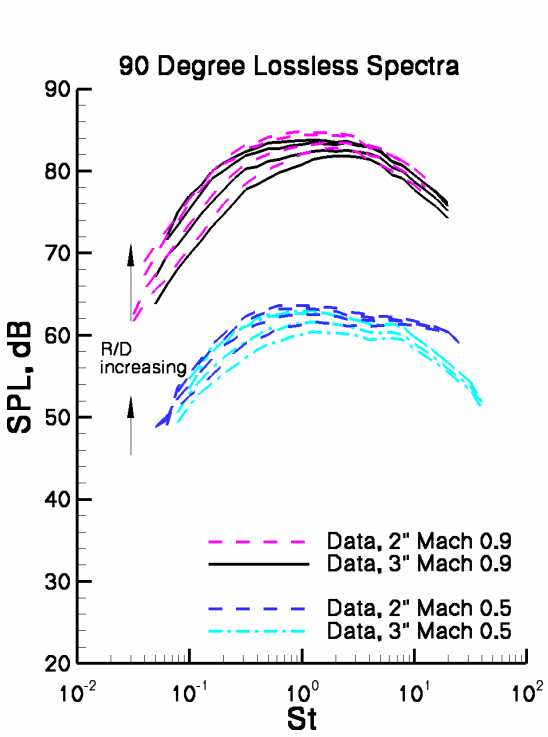

Figure 7.—Measured spectra at 90° scaled to 100 diameters using inverse square law

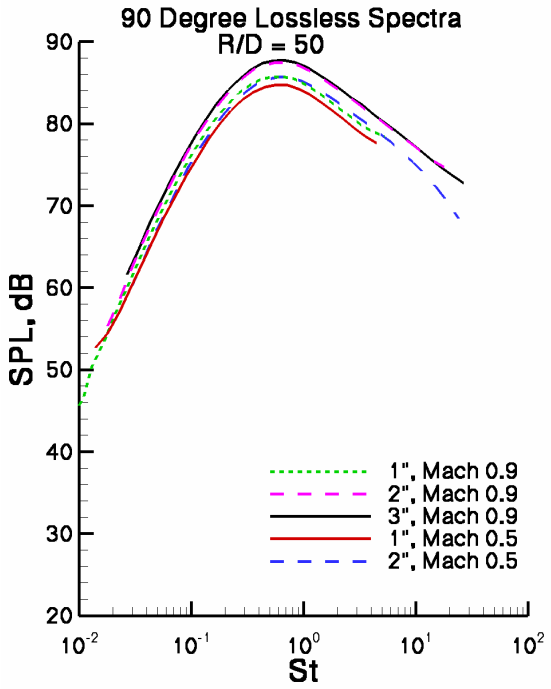

Figure 6.—Predicted spectra at 90° from Figure 5 additionally scaled for jet Mach number using the U^8 power law

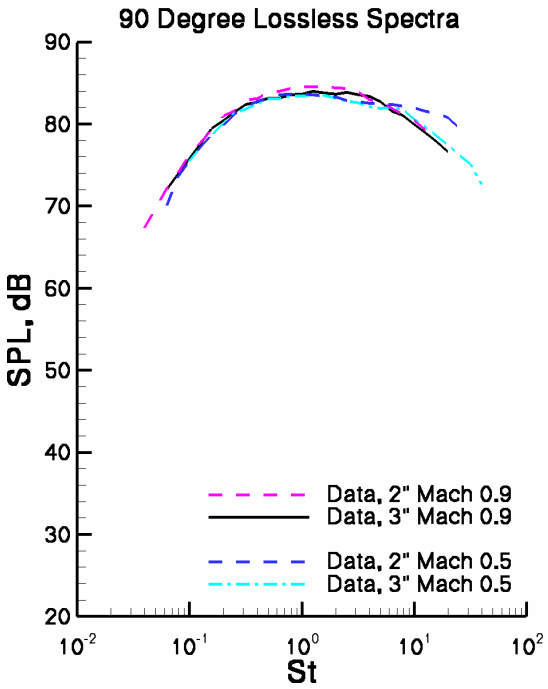

Figure 8.—Measured spectra at 90° from Figure 7 additionally scaled for jet Mach number using the U^8 power law

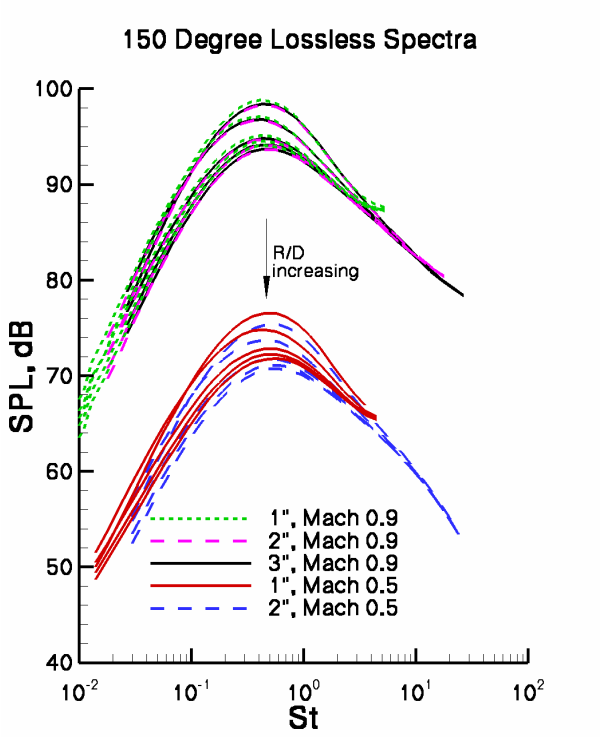

Figure 9.—Predicted spectra at 150° scaled to 100 diameters using inverse square law

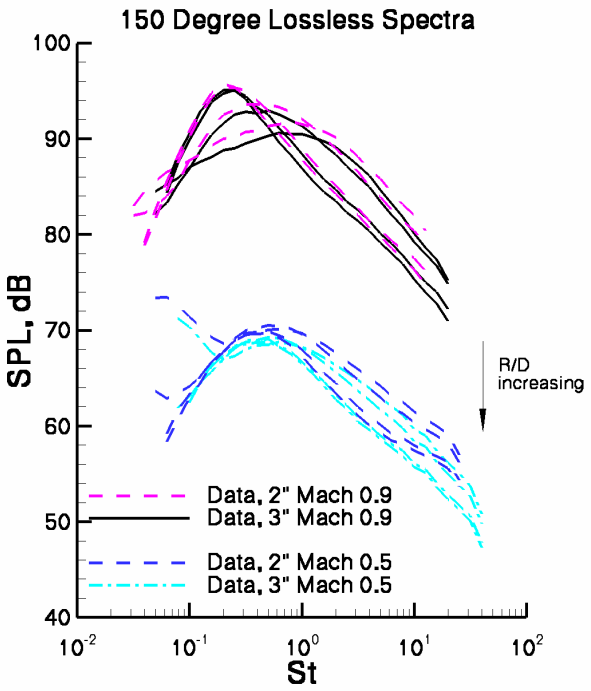

Figure 11.—Measured spectra at 150° scaled to 100 diameters using inverse square law

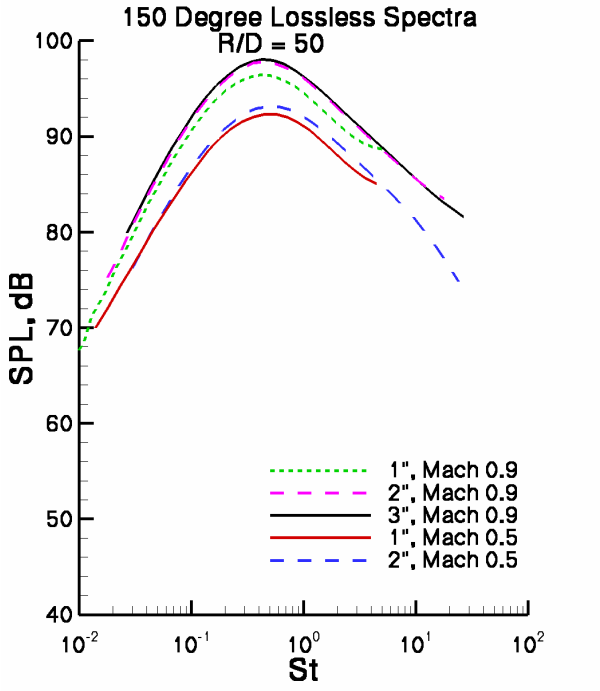

Figure 10.—Predicted spectra at 150° from Figure 9 additionally scaled for jet Mach number using the U^8 power law

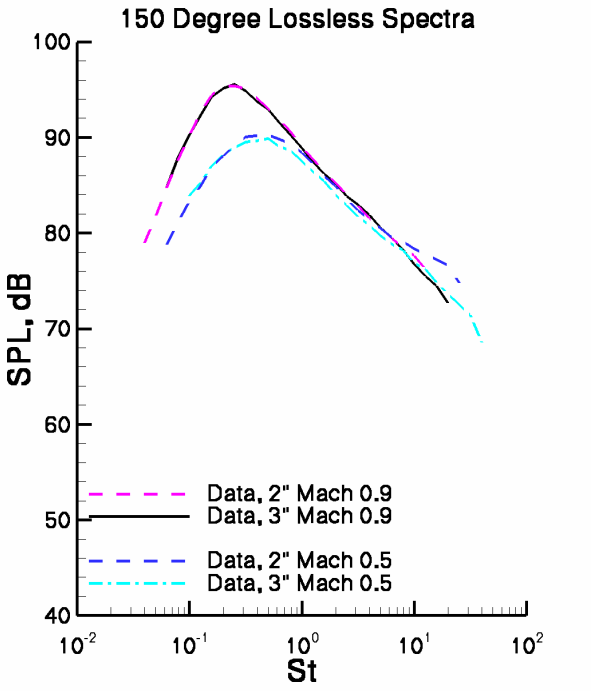

Figure 12.—Measured spectra at 150° from Figure 11 additionally scaled for jet Mach number using the U^8 power law

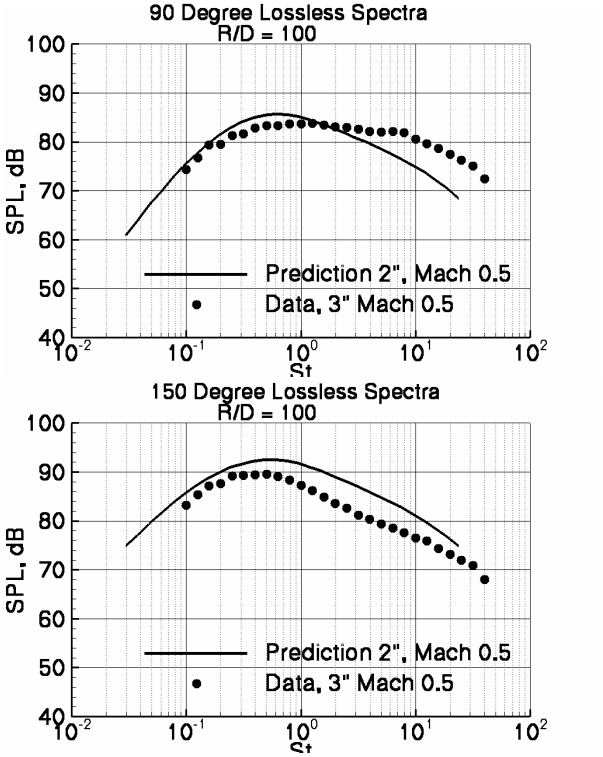

Figure 13.—Predicted and measured spectra at 90° and 150° scaled using the inverse-square law and the U^8 power law

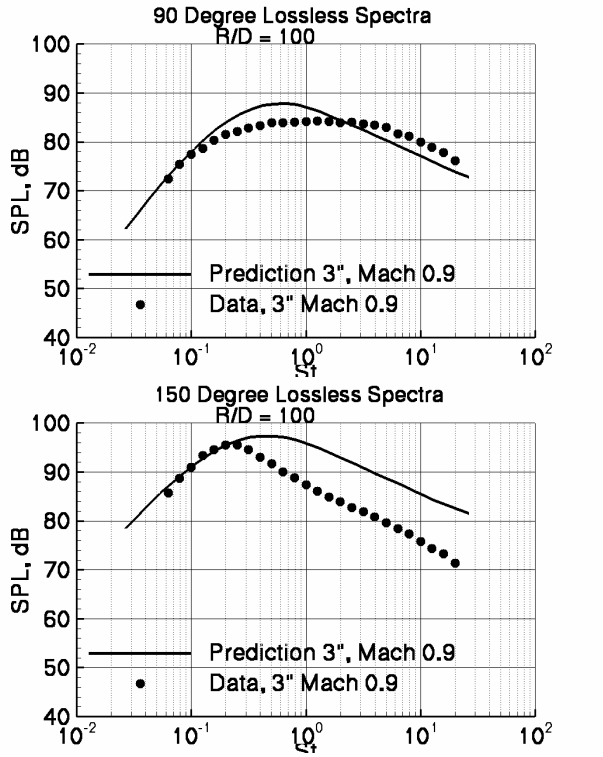

Figure 14.—Predicted and measured spectra at 90°and 150° scaled using the inverse-square law and the U^8 power law at Mach 0.9

REPORT DOCUMENTATION PAGE

Form Approved
OMB No. 0704-0188

1. AGENCY USE ONLY (*Leave blank*)	2. REPORT DATE	3. REPORT TYPE AND DATES COVERED
	May 2003	Technical Memorandum

4. TITLE AND SUBTITLE

Numerical and Experimental Determination of the Geometric Far Field for Round Jets

5. FUNDING NUMBERS

WBS–22–781–30–12

6. AUTHOR(S)

L. Danielle Koch, James Bridges, Cliff Brown, and Abbas Khavaran

7. PERFORMING ORGANIZATION NAME(S) AND ADDRESS(ES)

National Aeronautics and Space Administration
John H. Glenn Research Center at Lewis Field
Cleveland, Ohio 44135–3191

8. PERFORMING ORGANIZATION REPORT NUMBER

E–13956

9. SPONSORING/MONITORING AGENCY NAME(S) AND ADDRESS(ES)

National Aeronautics and Space Administration
Washington, DC 20546–0001

10. SPONSORING/MONITORING AGENCY REPORT NUMBER

NASA TM—2003-212379

11. SUPPLEMENTARY NOTES

Prepared for Noise-Con 2003 sponsored by the Institute of Noise Control Engineering of the USA (INCE-USA), Cleveland, Ohio, June 23–25, 2003. L. Danielle Koch, James Bridges, and Cliff Brown, NASA Glenn Research Center; Abbas Khavaran, QSS Group, Inc., Cleveland, Ohio 44135. Responsible person, L. Danielle Koch, organization code 5940, 216–433–5656.

12a. DISTRIBUTION/AVAILABILITY STATEMENT

Unclassified - Unlimited
Subject Categories: 02, 34, and 71 Distribution: Nonstandard

Available electronically at http://gltrs.grc.nasa.gov

This publication is available from the NASA Center for AeroSpace Information, 301–621–0390.

12b. DISTRIBUTION CODE

13. ABSTRACT ***(Maximum 200 words)***

To reduce ambiguity in the reporting of far field jet noise, three round jets operating at subsonic conditions have recently been studied at the NASA Glenn Research Center. The goal of the investigation was to determine the location of the geometric far field both numerically and experimentally. The combination of the WIND Reynolds-Averaged Navier-Stokes solver and the MGBK jet noise prediction code was used for the computations, and the experimental data was collected in the Aeroacoustic Propulsion Laboratory. While noise sources are distributed throughout the jet plume, at great distances from the nozzle the noise will appear to be emanating from a point source and the assumption of linear propagation is valid. Closer to the jet, nonlinear propagation may be a problem, along with the known geometric issues. By comparing sound spectra at different distances from the jet, both from computational methods that assume linear propagation, and from experiments, the contributions of geometry and nonlinearity can be separately ascertained and the required measurement distance for valid experiments can be established. It is found that while the shortest arc considered here (~8D) was already in the geometric far field for the high frequency sound (St >2.0), the low frequency noise due to its extended source distribution reached the geometric far field at or about 50D. It is also found that sound spectra at far downstream angles does not strictly scale on Strouhal number, an observation that current modeling does not capture.

14. SUBJECT TERMS	15. NUMBER OF PAGES
Navier-Stokes; Exhaust nozzles; Mixing; Turbulence; Aerodynamic noise	16
	16. PRICE CODE

17. SECURITY CLASSIFICATION OF REPORT	18. SECURITY CLASSIFICATION OF THIS PAGE	19. SECURITY CLASSIFICATION OF ABSTRACT	20. LIMITATION OF ABSTRACT
Unclassified	Unclassified	Unclassified	